Acceleration of the Healing Process and Myocardial Regeneration May Be Important as a Mechanism of Improvement of Cardiac Function and Remodeling by Postinfarction Granulocyte Colony–Stimulating Factor Treatment

Shinya Minatoguchi, MD; Genzou Takemura, MD; Xue-Hai Chen, MD; Ningyuan Wang, MD; Yoshihiro Uno, MD; Masahiko Koda, MD; Masazumi Arai, MD; Yu Misao, MD; Chuanjiang Lu, MD; Koji Suzuki, MD; Kazuko Goto, BSc; Ai Komada, BSc; Tomoyuki Takahashi, PhD; Kenichiro Kosai, MD; Takako Fujiwara, MD; Hisayoshi Fujiwara, MD

Background—We investigated whether the improvement of cardiac function and remodeling after myocardial infarction (MI) by granulocyte colony–stimulating factor (G-CSF) relates to acceleration of the healing process, in addition to myocardial regeneration.

Methods and Results—In a 30-minute coronary occlusion and reperfusion rabbit model, saline (S) or 10 μg · kg^{-1} · d^{-1} of human recombinant G-CSF (G) was injected subcutaneously from 1 to 5 days after MI. Smaller left ventricular (LV) dimension, increased LV ejection fraction, and thicker infarct-LV wall were seen in G at 3 months after MI. At 2, 7, and 14 days and 3 months after MI, necrotic tissue areas were 14.2±1.5/13.4±1.1, 0.4±0.1/1.8±0.5*, 0/0, and 0/0 mm^2 · slice^{-1} · kg^{-1}, granulation areas 0/0, 4.0±0.7/8.5±1.0*, 3.9±0.8/5.7±0.7,* and 0/0 mm^2 · slice^{-1} · kg^{-1}, and scar areas 0/0, 0/0, 0/0, and 4.2±0.5/7.9±0.9* mm^2 · slice^{-1} · kg^{-1} in G and S, respectively (*P<0.05, G versus S). Clear increases of macrophages and of matrix metalloproteinases (MMP) 1 and 9 were seen in G at 7 days after MI. This suggests that G accelerates absorption of necrotic tissues via increase of macrophages and reduces granulation and scar tissues via expression of MMPs. Meanwhile, surviving myocardial tissue areas within the risk areas were significantly increased in G despite there being no difference in LV weight, LV wall area, or cardiomyocyte size between G and S. Confocal microscopy revealed significant increases of cardiomyocytes with positive 3,3,3′,3′-tetramethylindocarbocyanine perchlorate and positive troponin I in G, suggesting enhanced myocardial regeneration by G.

Conclusions—The acceleration of the healing process and myocardial regeneration may play an important role for the beneficial effect of post-MI G-CSF treatment. (*Circulation.* 2004;109:2572-2580.)

Key Words: myocytes ■ ischemia ■ reperfusion ■ matrix metalloproteinase

G ranulocyte colony–stimulating factor (G-CSF), which can mobilize multipotential progenitor cells of bone marrow (BM) into peripheral blood, may improve post–myocardial infarction (MI) left ventricular (LV) remodeling and function. At present, the main mechanism is believed to be transdifferentiation of BM progenitor cells into the cell lineages of the heart, including cardiomyocytes, endothelial cells, etc, in the MI tissues.[1,2] However, recent studies have suggested that the transdifferentiation of c-Kit–positive BM cells into cardiomyocytes is controversial[3] and the number of the transdifferentiated cardiomyocytes from BM stem cells may be too low to explain the improvement of cardiac remodeling and function.[4]

The healing process after MI begins from absorption of necrotic tissues (acute stage: within several days after MI), moves into granulation with numerous myofibroblasts, rich microvessels, and collagen (subacute stage: 1 to 3 weeks after MI), and then forms scar tissues consisting primarily of collagen, with rare vessels via apoptosis of granulation cells (chronic stage: >1 month).[5] However, to the best of our knowledge, the precise quantitative studies on the dynamic changes of the above-described tissue factors are rare. Orlic et al[6] reported that scar tissue areas were reduced after G-CSF treatment, although the mechanism and the role were not examined. In the field of dermatology, it has been established that G-CSF enhances the

Circulation is available at http://www.circulationaha.org

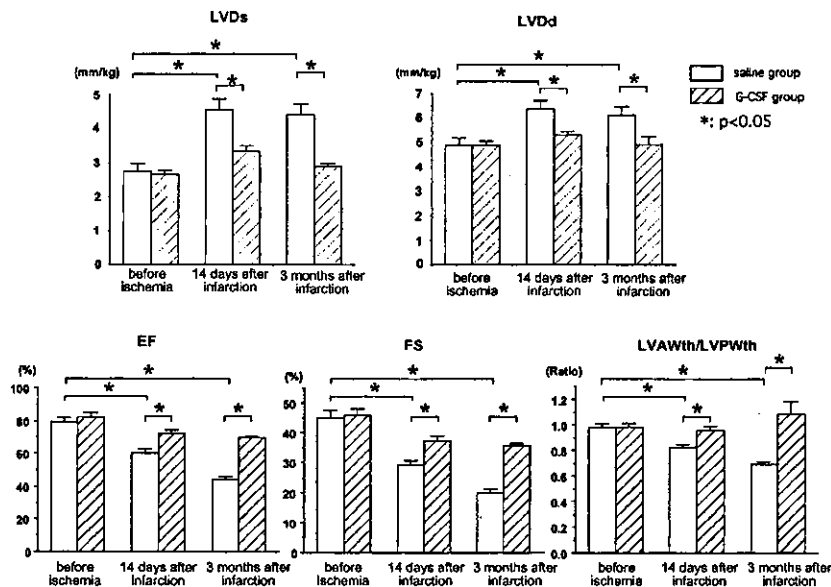DOI: 10.1161/01.CIR.0000129770.93985.3E

Figure 1. Echocardiographic data 14 days and 3 months after infarction. Note improvement of remodeling and function in G-CSF group. LVDs indicates LV systolic diameter; LVDd, LV diastolic diameter; EF, ejection fraction; FS, fractional shortening; LVAWth, LV anterior wall thickness; and LVPWth, LV posterior wall thickness.

healing process of various types of skin wounds via expression of various cytokines, such as the matrix metalloproteinase (MMP) family.[7–9] We hypothesized that G-CSF may also accelerate the healing process of MI wounds and that the acceleration may play an important role in the beneficial effects. Thus, the purpose of the present study was to define whether post-MI G-CSF treatment modifies the healing process via expression of MMPs, in addition to regeneration of myocardial tissues.

Methods

In this study, all rabbits received humane care in accordance with the *Guide for the Care and Use of Laboratory Animals*, published by the US National Institutes of Health (NIH publication 8523, revised 1985). The study protocol was approved by the Ethical Committee of Gifu University School of Medicine, Gifu, Japan.

The standard methods of 30-minute coronary arterial occlusion and reperfusion in male Japanese White rabbits weighing 1.9 to 2.2 kg were performed as previously reported.[10] Briefly, under anesthesia and mechanical ventilation with room air, a left thoracotomy was performed, and 4-0 silk string was placed beneath the large coronary arterial branch coursing down the middle of the anterolateral surface of the left ventricle. Then, the rabbits were killed by an overdose of pentobarbital after heparinization (500 U/kg).

Protocol 1

The subjects were 120 rabbits with 30-minute ischemia and 2-day, 7-day, 14-day, or 3-month reperfusion as described above. Saline at 0.5 mL in the saline group or 10 μg · kg^{-1} · d^{-1} of recombinant human G-CSF (Lenograstin, Chugai Pharmaceutical Co, Ltd, Tokyo, Japan) in the G-CSF group starting 24 hours after infarction once per day for 5 days was administered subcutaneously in the 7-day groups (n=15 each in the saline and G-CSF groups), the 14-day groups (n=15 in each), and the 3-month groups (n=15 in each), but that in the 2-day groups (n=15 in each) was administered only once at 24 hours after infarction, when each rabbit was enrolled in the saline or G-CSF group by lot.

Echocardiography

Echocardiography (SSD2000, Aloka Co Ltd) and the measurement of arterial blood pressure were performed before and 14 days after MI in the 14-day groups (n=15 in each of the saline and G-CSF groups) and before and 3 months after MI in the 3-month groups (n=15 in each). The measurements were performed by 2 persons blinded to treatment.

Blood Sampling

Blood samples (0.3 mL each) were taken from an ear vein before and 7 days after MI in the 7-day groups (n=15 each in the saline and G-CSF groups) and before and 14 days after MI in the 14-day groups (n=15 in each) for peripheral blood cell counts and hemograms.

Pathology

The excised hearts of a total of 120 rabbits were mounted on a Langendorff apparatus, and Evans blue dye at 4°C was injected for 1 minute from the aorta after reocclusion of the coronary branch by a silk string for the measurement of risk areas. Then, the whole heart was perfused with 10% buffered formalin (4°C) for 2 minutes. The LV was weighed and sectioned into ≈7 transverse slices parallel to the atrioventricular ring. Each slice was fixed with 10% buffered formalin for 4 hours, embedded in paraffin, and sectioned with a microtome (4 μm thick). These sections were stained with hematoxylin-eosin and Sirius red. Under light microscopy, the risk area without blue dye, nonrisk area with blue dye, necrotic areas, granulation areas, and scar areas were clearly demarcated on the above-described stained preparations.

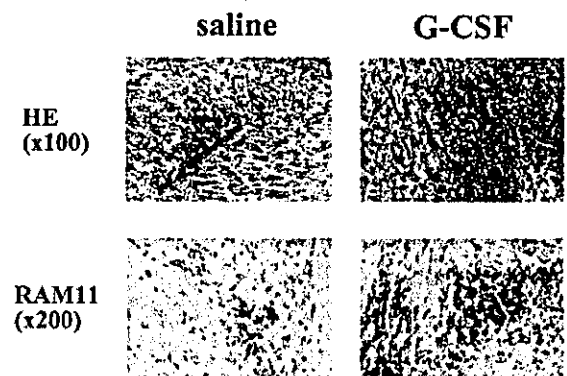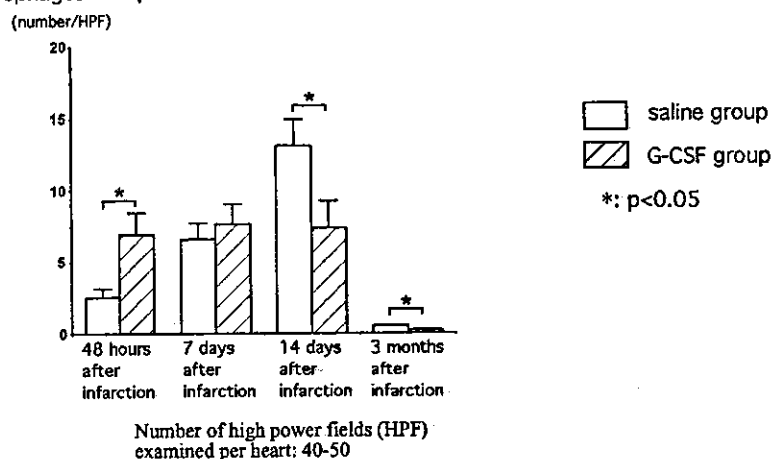## 48 hours after myocardial infarction

Figure 2. Histology of border zone between surviving area (left) and infarction (right). Note that acute inflammatory cell infiltration by hematoxylin-eosin (HE) stain and number of macrophages with positive RAM 11 stained with brown are clearly greater in G-CSF group.
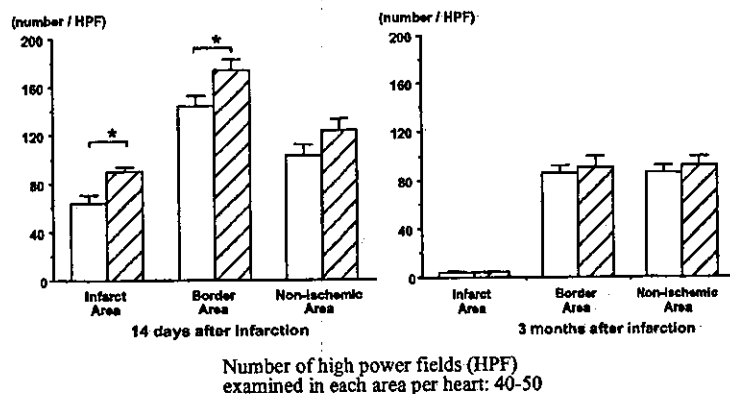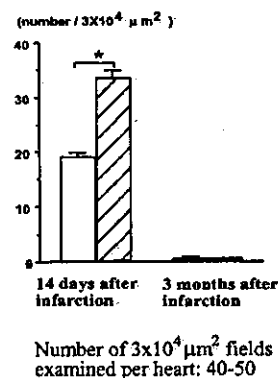
Figure 3. Quantitative analyses of macrophages, endothelial cells, and myofibroblasts

On the transversely sliced preparations with infarction in each heart, LV wall area, risk area, necrotic areas, granulation areas, scar areas, infarct areas, surviving areas in the risk areas, and collagen areas with positive Sirius red were calculated by use of an image analyzer connected to a light microscope (Luzex-F, Nireco) and were expressed as mm²/slice/body weight (kg) corrected by mean risk area of each group for precise comparison. These were performed by 2 persons blinded to treatment.

Immunohistochemistry

By use of an indirect immunoperoxidase method, immunohistochemical stainings were performed using monoclonal mouse anti-troponin I antibody (Chemicon International, Inc) at 1:10, monoclonal mouse anti-human CD31, endothelial cell antibody (Dako) at 1:100, monoclonal mouse anti-human α-smooth muscle actin (Dako smooth muscle actin, 1A4) at 1:250, monoclonal mouse anti-macrophage antibody (Dako RAM11) at 1:100 and monoclonal mouse anti-human MMP1 antibody (Daiichi Fine Chemical Co Ltd, F-67) at 1:400, each of which cross-reacts with rabbit tissues. Morphometric analyses were performed by 2 persons blinded to treatment.

Protocol 2

In 14 rabbits, BM (≈10 mL) was aspirated from the right and left iliac crests 2 days before ischemia-reperfusion. To evaluate the incorporation of BM cells into the myocardium, BM mononuclear cells were labeled with fluorescent carbocyanine 1,1'-dioctadecyl-1-3,3,3',3'-tetramethylindocarbocyanine perchlorate (DiI).[11] The DiI-labeled autologous BM mononuclear cells (≈1×10⁷ cells) were returned into the BM space in the right and left iliac crests of each rabbit. Two days later, 30-minute ischemia and reperfusion was performed. Then, the saline group (n=7) and the G-CSF group (n=7) were made up by the same method as shown above and killed 14 days after MI. In addition, 7 other rabbits, as a negative control in which non–DiI-labeled BM cells were returned to BM of iliac crests, were killed 14 days after MI.

The hearts excised 14 days after MI were placed in iced PBS at <4°C immersion immediately after the animals were killed. The tissues (≈3×3×2 mm each) obtained from the risk area, including MI, and from the nonrisk area (3 tissues each) of each heart were embedded in OCT compound (Miles Scientific) and snap-frozen in liquid nitrogen. The OCT compound tissues were sectioned at 4-μm thickness with a cryostat for immunohistochemical analysis. In addition, the BMs of iliac crests were examined immunohistochemically.

Immunohistochemical staining was performed with Hoechst 33342 for nuclear staining, in addition to those detailed above. These were observed with confocal microscopy (LSM510 NLO, Zeiss), which can simultaneously analyze the relation among 3 different fluorescences and phase-contrast illustration. Morphometric analyses were performed by 2 persons blinded to treatment.
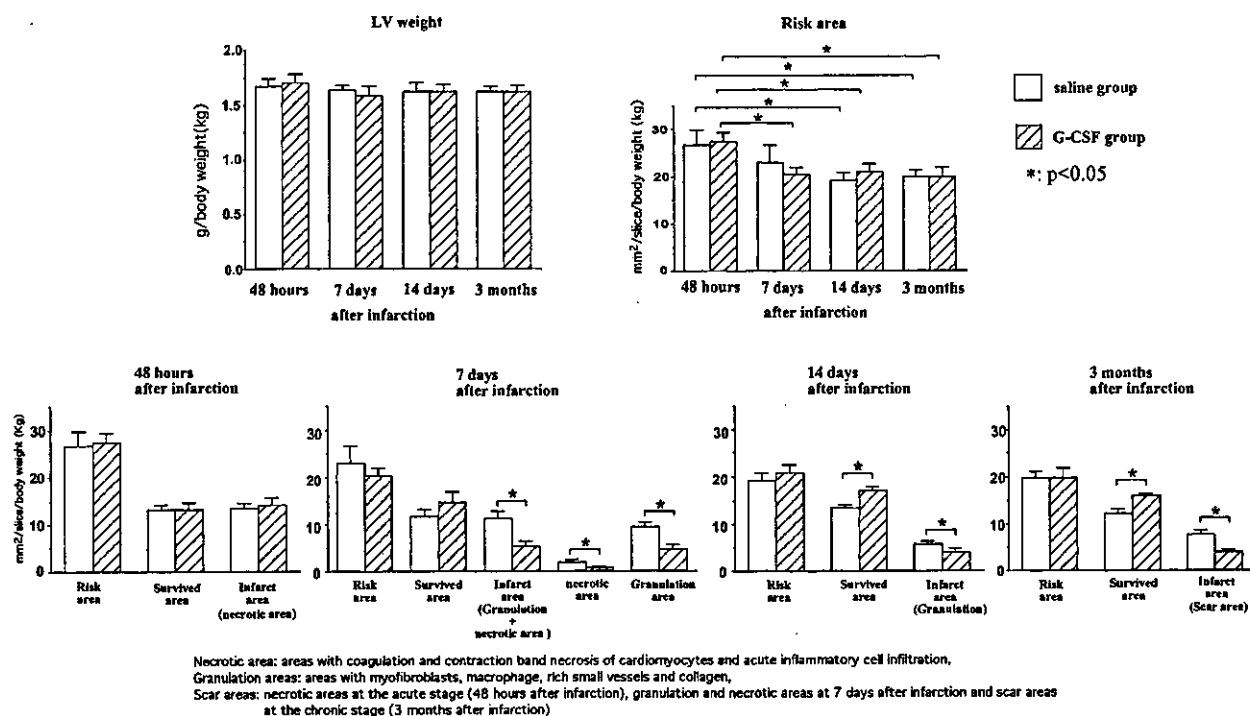
Necrotic area: areas with coagulation and contraction band necrosis of cardiomyocytes and acute inflammatory cell infiltration,
Granulation areas: areas with myofibroblasts, macrophage, rich small vessels and collagen,
Scar areas: necrotic areas at the acute stage (48 hours after infarction), granulation and necrotic areas at 7 days after infarction and scar areas
at the chronic stage (3 months after infarction)

Figure 4. Time-course changes of LV weight, risk area, surviving area, infarct area, necrotic area, granulation area, and scar area after infarction

Protocol 3

Other saline (n=7) and G-CSF (n=7) groups with 30-minute ischemia and 7-day reperfusion and a sham group (n=7) were prepared for the measurement of MMP-1 and 9. The excised hearts were placed in iced PBS at <4°C immersion immediately after the animals were killed. Tissues of ≈200 mg each obtained from the center of the risk area and from the nonrisk area of LV wall were snap-frozen in liquid nitrogen.

For the measurement of MMP-1, a collagenase, ≈50 mg of the above-described frozen tissues obtained from each heart of the sham, saline, and G-CSF groups, was homogenized in lysis buffer and centrifuged at 10 000g at 4°C for 10 minutes. MMP-1 was measured by Western blot analysis using anti-human MMP-1 mouse monoclonal antibody (Daiichi Fine Chemical Co, F-67, clone No. 41-1E5). The signals were quantified by densitometry. The measurement of MMP-9, a gelatinase, in the remaining samples of the above-described frozen tissues was performed by zymography using the recommended methods of the Gelatinzymo electrophoresis kit (Yagai Research Center).

Statistical Analysis

All values are presented as mean±SEM. The differences between the saline and G-CSF groups were assessed by 2-way repeated-measures ANOVA. Differences at $P<0.05$ were considered statistically significant.

Results

Mortality

All rabbits in the 3-month saline and G-CSF groups enrolled 24 hours after MI survived during 3 months of experimentation.

Echocardiography and Blood Pressure

As shown in Figure 1, echocardiography showed a significant decrease in the LV end-systolic and LV end-diastolic dimensions and significant increases in the LV ejection fraction and

fractional shortening in the G-CSF group compared with those of the saline group at 14 days and 3 months after MI. The ratio of the anterior LV wall thickness with infarction to the posterior wall thickness without infarction was greater in the G-CSF group than in the saline group. These suggest the improvements of LV remodeling and function by G-CSF. There was no significant difference in heart rate or blood pressure between the 2 groups (data not shown).

Peripheral Blood Cell Counts

White blood cells, granulocytes, and monocytes increased from 8800±588, 4021±278, and 357±91 before MI to 19 537±2641, 12 076±2663, and 1351±196/μL at 7 days after MI in the G-CSF group and were restored to 10 363±764, 5106±575, and 449±115/μL at 14 days after MI, respectively. There was no significant change in lymphocytes, red blood cells, or thrombocytes throughout the experiment. The saline group showed no significant changes.

General Histology

At 2 days after MI, large necrotic tissue areas were surrounded by numerous acute inflammatory cell infiltrations consisting of neutrophils, lymphocytes, and macrophages with positive RAM 11 in both the saline and G-CSF groups. However, the extent and density were clearly greater in the G-CSF group than in the saline group (Figure 2).

At 7 days after MI, necrotic tissue areas became smaller and acute infiltrated inflammatory cells were markedly reduced compared with the 2-day groups. The MI areas were to a large extent replaced by granulation in both the saline and G-CSF groups. At 14 days after MI, necrotic tissues were

Collagen Areas With Positive Sirius-Red

Myocyte size

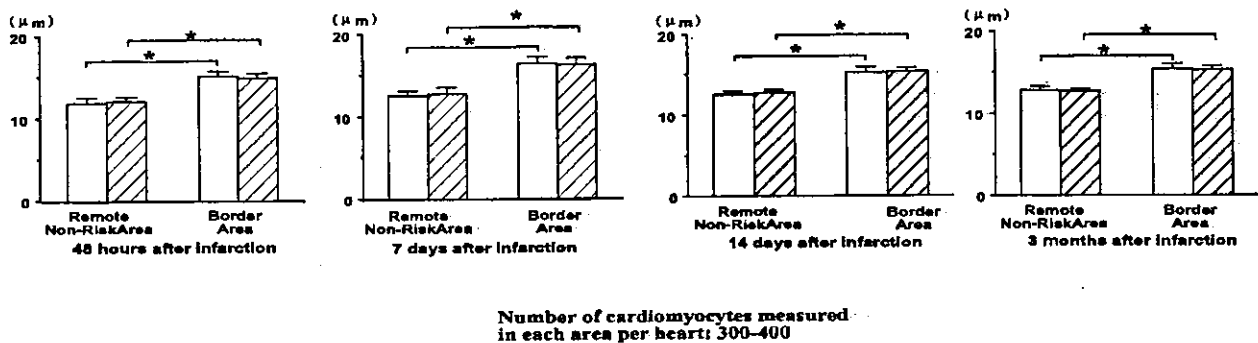Number of cardiomyocytes measured
in each area per heart: 300–400
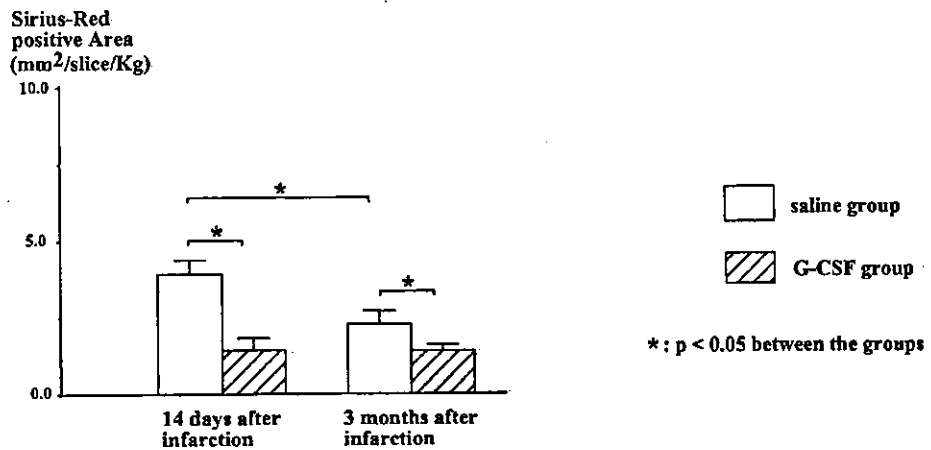
Figure 5. Collagen area with positive Sirius red and transverse size of cardiomyocytes

completely absorbed, and granulation tissues alone were observed in the saline and G-CSF groups. The densities of the myofibroblasts with positive α-smooth muscle actin and vessels with positive CD31 were clearly increased in the G-CSF group compared with those of the saline groups (Figure 3). The number of macrophages with positive RAM 11 was increased in the saline groups according to the duration of 2, 7, and 14 days (Figure 3). Meanwhile, it was similar in the G-CSF groups among the 3 durations. Thus, the number of macrophages was significantly greater in the G-CSF group than the saline group at 2 days after MI, similar at 7 days after MI, and lower in the G-CSF group than in the saline group at 14 days after MI (Figure 3).

At 3 months after MI, the granulation tissues were replaced by scar in each of the saline and G-CSF groups. The number of macrophages became small in each of the G-CSF and saline groups (Figure 3). However, it was significantly lower in the G-CSF group than the saline group.

Risk Area, Necrotic Area, Granulation Tissue Area, Scar Tissue Area, Collagen Area, Surviving Area, and Size of Cardiomyocytes

Among the 2-day, 7-day, 14-day, and 3-month groups, there were no significant differences of LV weights, LV areas, and nonrisk areas in any of the G-CSF and saline groups (Figure 4). The risk areas were significantly reduced in each of the G-CSF and saline groups at 14 days and 3 months after MI, compared with those at 2 days after MI, although the risk areas at 2 days after MI were similar between the G-CSF and saline groups (Figure 4).

The MI areas at 2 days after MI (necrotic tissue areas) were similar between the G-CSF and saline groups. However, they were reduced slightly in the saline groups and markedly in the G-CSF groups at 7 days (necrotic areas + granulation areas), 14 days (granulation areas), and 3 months (scar areas) after MI (Figure 4). The differences between the G-CSF and saline groups were significant. The necrotic areas, which were similar between the G-CSF and saline groups at 2 days after MI, were reduced moderately in the saline group and markedly in the G-CSF group at 7 days after MI (Figure 4). The difference between the 2 groups was significant. The granulation areas at 7 and 14 days after MI were significantly smaller in the G-CSF groups than the saline groups (Figure 4). In addition, the scar areas at 3 months after MI were significantly smaller in the G-CSF group than the saline group (Figure 4). Collagen areas with positive Sirius red
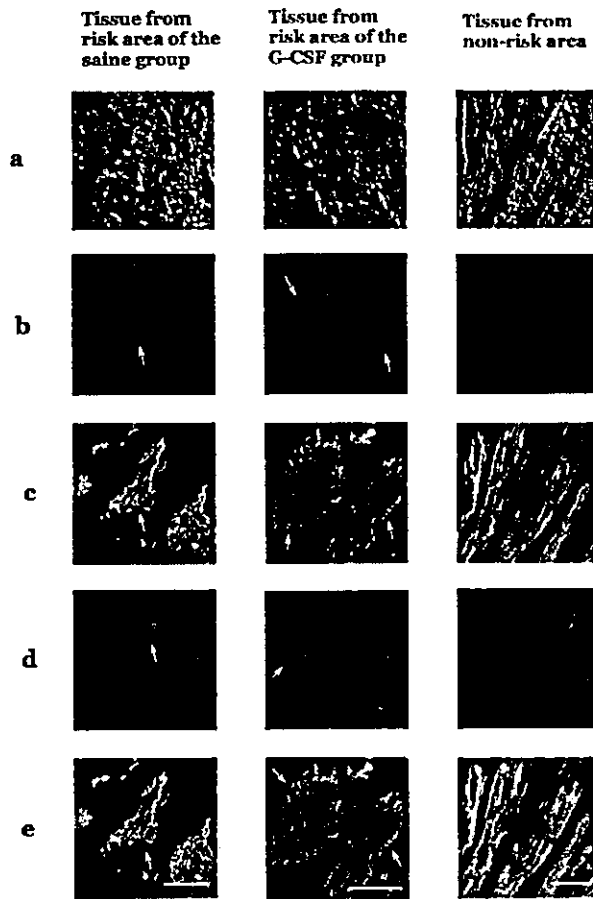
Tissue from risk area of the saine group	Tissue from risk area of the G-CSF group	Tissue from non-risk area

a

b

c

d

e

Figure 6. Confocal microscopic findings 14 days after infarction. Cells with positive DiI, an indicator of BM-derived cells, and positive troponin I, an indicator of cardiomyocytes, are observed in both saline and G-CSF groups. Note greater number in G-CSF group.

staining were significantly smaller in the G-CSF groups than the saline groups at 14 days and 3 months after MI (Figure 5).

The surviving areas of the saline groups within the risk areas were similar at 2 days, 7 days, 14 days, and 3 months after MI (Figure 4). However, those of the G-CSF groups were significantly larger at 14 days and 3 months after MI compared with that at 2 days after MI. The difference between the G-CSF and saline groups was significant at 14 days and 3 months after MI.

The transverse size of cardiomyocytes in the border zone between the surviving and infarct areas was significantly greater than that of the nonrisk areas in the G-CSF and saline groups even 2 days after MI (Figure 5). However, the sizes were similar between the saline and G-CSF groups and among 2 days, 7 days, 14 days, and 3 months after MI (Figure 5).

DiI-Labeled Cells

Confocal microscopy revealed the DiI-labeled cells with positive troponin I, a specific marker of cardiomyocytes (Figure 6); CD31, a marker of endothelial cells; or α-smooth muscle actin in the myocardial tissues obtained from the risk

area but not in the tissues from the nonrisk area in the saline and G-CSF groups 14 days after MI (Figure 7). The DiI-labeled cells with positive α-smooth muscle actin were seen in the small vessels, indicating smooth muscle cells, and in the extravascular areas, indicating myofibroblasts (Figure 7). The percentages of DiI-labeled cells in troponin I–positive cells were significantly increased in the G-CSF group (0.13±0.03% versus 0.05±0.02% of the saline group). The percentages of DiI-labeled cells in CD31-positive cells and α-smooth muscle actin–positive cells were significantly increased in the G-CSF group (6.9±1.7 and 5.4±1.6% versus 3.3±1.1 and 1.7±0.7% of the saline group, respectively).

In the BM of iliac crests, DiI-positive cells with nuclei showed a scattered distribution (Figure 7), suggesting the reconstruction of the injected BM cells.

MMP Expression

MMP 1 was significantly increased in the risk area of the saline and G-CSF groups and in the nonrisk area of the G-CSF group compared with that of the sham group (Figure 8). It was greatest in the risk area of the G-CSF group. MMP 9 was significantly increased in the risk area and nonrisk area of the G-CSF group.

Discussion

Acceleration of the Postinfarction Healing Process by G-CSF

The present study revealed that necrotic tissue areas as acute MI size were similar in the G-CSF and saline groups 2 days after MI but were smaller in the G-CSF group 7 days after MI. At 2 days after MI, the numbers of infiltrated neutrophils and macrophages in the acute MI areas, which have strong phagocytosis, were definitely increased in the G-CSF group. Therefore, the prompt absorption of necrotic tissues by G-CSF may be related to the enhanced mobilization of neutrophils and macrophages from BM.

Granulation, scar, and collagen areas were smaller in the G-CSF groups than the saline groups. MMP 1, a collagenase, and MMP 9, a gelatinase, were overexpressed in the G-CSF groups. This is similar to previous findings that G-CSF enhances the MMP family in cancer and blood cells.[12,13] Therefore, the reducing effect of collagen by G-CSF may be related to overexpression of the MMP family. Many studies showed that G-CSF improves the healing process of skin wounds such as doxorubicin-induced skin necrosis and burn injury of animal models and infected ulcers of the foot in patients with diabetes mellitus.[7–9] Improvement of immuno-compromised states by G-CSF has been suggested.[8] This is supported by the lower level of macrophages at the subacute and chronic stages in the present study. Thus, post-MI G-CSF treatment accelerates the healing process of MI wounds.

Regeneration of Myocardial Tissues by G-CSF

At present, progenitor cells of cardiomyocytes, in addition to those of endothelial cells and smooth muscle cells, may be present in the myocardium itself, as in the BM. To define whether MI alone and G-CSF can mobilize BM-derived progenitor cells from BM into the heart, BM mononuclear cells labeled with DiI were returned into BM of the iliac

Myocardial infarct tissues

Bone marrow in iliac crest

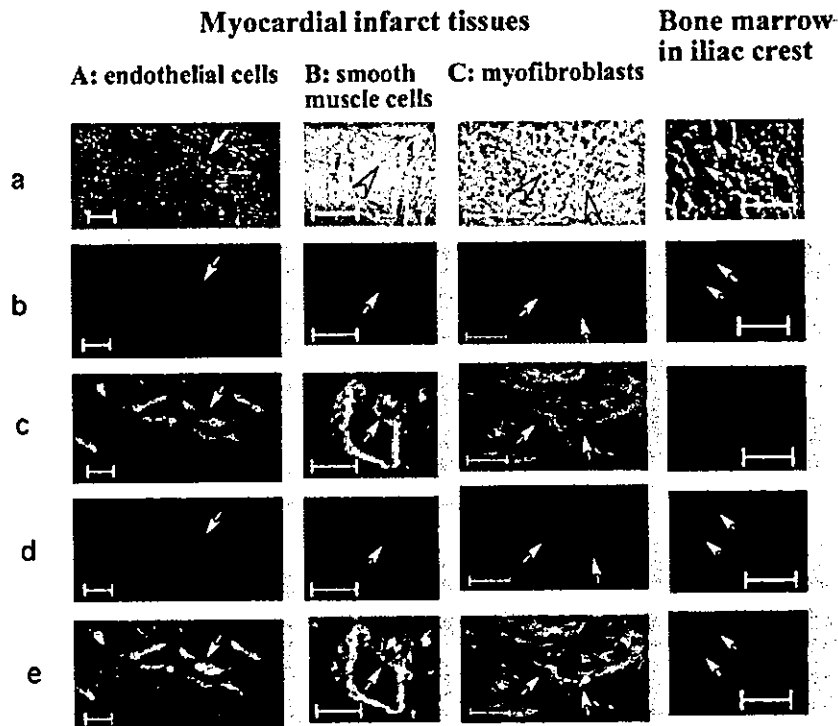A: endothelial cells   B: smooth muscle cells   C: myofibroblasts

Figure 7. Confocal microscopic findings of saline group 14 days after infarction. Note presence of BM (BM)-derived endothelial cells, smooth muscle cells and myofibroblasts shown by arrows. Also note reconstruction of BM cells injected into iliac crest.

crests. DiI-positive and troponin I–, CD31-, or α-smooth muscle actin–positive cells, suggesting the transdifferentiated cardiomyocytes, endothelial cells, or smooth muscle cells (or myofibroblasts), respectively, were seen in the risk areas of the saline and G-CSF groups. The percentages were increased by G-CSF treatment. Thus, MI itself may induce regeneration of myocardial cells via mobilization of BM stem cells, and G-CSF may enhance the process.

However, several recent in vivo studies reported the presence of fusion between cardiomyocytes and BM progenitor cells.[14] In the present study, we cannot deny its possibility. In addition, the number of regenerated cells mobilized from the BM of the whole body is unknown because of the methodological limitations of the present study. However, surviving myocardial tissue areas within the risk areas in the G-CSF groups were increased 14 days and 3 months after MI. The transverse size of cardiomyocytes within the risk areas was similar between the G-CSF and saline groups. Death of cardiomyocytes is determined within several hours after reperfusion. In the present study, the first G-CSF injection was performed 24 hours after reperfusion, and acute infarct size at 2 days after reperfusion was similar between the G-CSF and saline groups. Therefore, it is considered that cell fusion caused by G-CSF therapy may occur between the BM cells and surviving cardiomyocytes in the risk areas, but it could not rescue the cardiomyocyte death in the present study. This suggests that an increase of surviving myocardial tissue areas by G-CSF is a result of regeneration of myocardial tissues, including cardiomyocytes. A part of the cells in the regenerated myocardial tissues may originate from BM progenitor cells. There is a possibility that hematopoietic stem cells are involved in the progenitor cells that were responsible for myocardial regeneration, because G-CSF generally mobilizes hematopoietic stem cells.

Mechanism of Improvement of LV Remodeling and Function by G-CSF

First, the enhanced myocardial tissue regeneration would contribute to the beneficial effects as detailed previously.[6] Second, rapid absorption of necrotic tissues relating to the higher level of neutrophils and macrophages at the acute stage and improvement of chronic inflammation suggested by the lower level of macrophages at the subacute and chronic stages may contribute to the beneficial effects. Third, production of fibrosis after MI prevents structural fragility. Previous studies reported that a MMP family was increased in the postinfarction heart failure models with permanent occlusion and large infarction and that the inhibitors beneficially affected cardiac remodeling and function.[15,16] Thus, it is suggested that an increase in MMP has an aggravating effect on heart failure via collagen degradation. However, it is well known that the volume of reactive granulation and/or scar tissues after skin injury after burn, surgery, etc, frequently becomes excessive, and this is called hypertrophic scarring. The excessive extent of fibrosis without contractility or relaxation would accelerate cardiac remodeling and decrease cardiac function, as seen in ischemic or idiopathic dilated cardiomyopathy. In such cases, an increase in the MMP family may be one of the protective mechanisms via proteolysis of excessive collagen. In fact, this concept is supported by findings of several previous studies: an inhibition of MMP caused cardiac failure,[17] targeted deletion of MMP 9 attenuated LV remodeling and collagen accumulation via overexpression of MMP-2 and MMP-13,[18] and an increase in

Western blot analysis

Zymographic analysis

SN=non-risk area in the saline group, SI=infarct area in the saline group,
GN=non-risk area in the G-CSF group, GI=infarct areain the G-CSF group, *: $p<0.05$

Immunohistochemical analysis of MMP-1
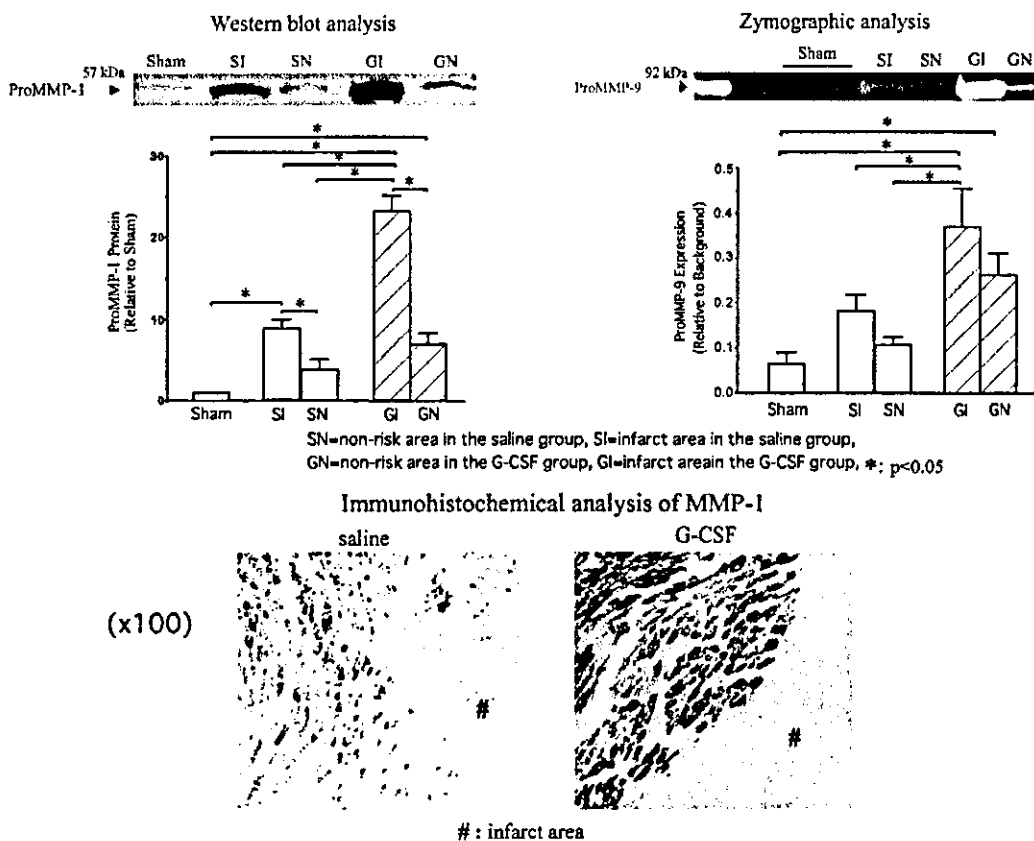
saline   G-CSF

(x100)

: infarct area

Figure 8. MMP 1 and 9 at 7 days after infarction. Note overexpression of MMP 1 and 9 in G-CSF group. MMP 1 was expressed in cardiomyocytes surrounding infarct area, and expression was greater in G-CSF group.

MMP-1 by hepatocyte growth factor was beneficial on post-MI heart failure via its anti-fibrotic action;[19] reduction of scar tissue and improvement of remodeling were observed simultaneously in myocardial regeneration therapy.[1,6] An adequate content of fibrosis may be different because of the various conditions of MI models, such as small or large MI, small or large amount of myocardial regeneration, and permanent or transient ischemia. Thus, in the present model with transient ischemia and nonlarge infarction, the beneficial effect of G-CSF relies on a higher number of migrated neutrophils/macrophages and upregulation of MMPs and increased participation of mobilized stem cells, which supports the concept of myocardial repair after infarction by Orlic et al.[6] Also, further investigation using MMP gene-defective mice or mice with blocking antibody would be warranted to define the precise role of MMP.

Clinical Implications

The standard therapy for human MI is reperfusion therapy, and our study showed the beneficial effect of G-CSF using a reperfusion model. The dose of G-CSF and the increased level in peripheral leukocytes were similar to those in a normal human donor for BM transplantation.[20] In addition to modification of the healing process and regeneration of myocardial tissues, this would offer the important suggestion of using the clinical application of G-CSF as a noninvasive therapy.

Conclusions

Both the acceleration of the healing process and myocardial regeneration play an important role in the beneficial effects of G-CSF.

References

1. Orlic D, Kajstura J, Chimenti S, et al. Bone marrow cells regenerate infarcted myocardium. *Nature.* 2001;410:701–705.
2. Asahara T, Masuda H, Takahashi T, et al. Bone marrow origin of endothelial progenitor cells responsible for postnatal vasculogenesis in physiological and pathological neovascularization. *Circ Res.* 1999;85: 221–228.
3. Wagers AJ, Sherwood RI, Christensen JL, et al. Little evidence for developmental plasticity of adult hematopoietic stem cells. *Science.* 2002; 297:2256–2259.
4. Taylor DA, Hruban R, Rodriguez ER, et al. Cardiac chimerism as a mechanism for self-repair: does it happen and if so to what degree? *Circulation.* 2002;106:2–4.
5. Takemura G, Ohno M, Hayakawa Y, et al. Role of apoptosis in the disappearance of infiltrated and proliferated interstitial cells after myocardial infarction. *Circ Res.* 1998;82:1130–1138.
6. Orlic D, Kajstura J, Chimenti S, et al. Mobilized bone marrow cells repair the infarcted heart, improving function and survival. *Proc Natl Acad Sci U S A.* 2001;98:10344–10349.
7. Vargel I, Erdem A, Ertoy D, et al. Effects of growth factors on doxorubicin-induced skin necrosis: documentation of histomorphological

alterations and early treatment by GM-CSF and G-CSF. *Ann Plastic Surg.* 2002;49:646–653.

8. Peter FW, Schuschke DA, Barker JH, et al. The effect of severe burn injury on proinflammatory cytokines and leukocyte behavior: its modulation with granulocyte colony stimulating factor. *Burns.* 1999;25:477–486.

9. Gough A, Clapperton M, Rolando N, et al. Randomised placebo-controlled trial of granulocyte-colony stimulating factor in diabetic foot infection. *Lancet.* 1997;350:855–859.

10. Minatoguchi S, Arai S, Uno Y, et al. Anti-diabetic drug, miglitol, markedly reduces myocardial infarct size in rabbits. *Br J Pharmacol.* 1999;128:1667–1672.

11. Kalka C, Masuda H, Takahashi T, et al. Transplantation of ex vivo expanded endothelial progenitor cells for therapeutic neovascularization. *Proc Natl Acad Sci U S A.* 2000;97:3422–3429.

12. Sugimoto C, Fujieda S, Sunaga H, et al. Granulocyte colony-stimulating factor (G-CSF)-mediated signaling regulates type IV collagenase activity in head and neck cancer cells. *Int J Cancer.* 2001;93:42–46.

13. Carstanjen D, Ulbricht N, Lacone A, et al. Matrix metalloproteinase-9 (gelatinase B) is elevated during mobilization of peripheral blood progenitor cells by G-CSF. *Transfusion.* 2002;42:588–596.

14. Alvarez-Dolado M, Pardal R, Garcia-Verdugo JM, et al. Fusion of bone-marrow-derived cells with Purkinje neurons, cardiomyocytes and hepatocytes. *Nature.* 2003;425:968–973.

15. Spinale FG. Matrix metalloproteinases: regulation and dysregulation on the failing heart. *Circ Res.* 2002;90:520–530.

16. Creemers EEJM, Cleutjens JPM, Smits JFM, et al. Matrix metalloproteinase inhibition after myocardial infarction: a new approach to prevent heart failure? *Circ Res.* 2001;89:201–210.

17. Heymans S, Luttun A, Nuyens D, et al. Inhibition of plasminogen activators or matrix metalloproteinases prevents cardiac rupture but impairs therapeutic angiogenesis and causes cardiac failure. *Nat Med.* 1999;5: 1135–1142.

18. Ducharme A, Frantz S, Aikawa M, et al. Targeted deletion of matrix metalloproteinase-9 attenuates left ventricular enlargement and collagen accumulation after experimental myocardial infarction. *J Clin Invest.* 2000;106:55–62.

19. Taniyama Y, Morishita R, Nakagami H, et al. Potential contribution of a novel antifibrotic factor, hepatocyte growth factor, to prevention of myocardial fibrosis by angiotensin II blockade in cardiomyopathic hamsters. *Circulation.* 2000;102:246–252.

20. Kroger N, Renges H, Kruger W, et al. A randomized comparison of once versus twice daily recombinant human granulocyte colony-stimulating factor (Filgrastim) for stem cell mobilization in healthy donors for allogeneic transplantation. *Br J Haematol.* 2000;111: 761–765.

/3

npg

Local overexpression of HB-EGF exacerbates remodeling following myocardial infarction by activating noncardiomyocytes

Hiroaki Ushikoshi[1,2], Tomoyuki Takahashi[1,4], Xuehai Chen[2], Ngin Cin Khai[1], Masayasu Esaki[1,2], Kazuko Goto[1], Genzou Takemura[2], Rumi Maruyama[2], Shinya Minatoguchi[2], Takako Fujiwara[3], Satoshi Nagano[1,4], Kentaro Yuge[1], Takao Kawai[1,2], Yoshiteru Murofushi[1,4], Hisayoshi Fujiwara[2] and Ken-ichiro Kosai[1,4]

[1]Department of Gene Therapy and Regenerative Medicine, Gifu University School of Medicine, Gifu, Japan; [2]Department of Cardiology, Respirology and Nephrology, Regeneration & Advanced Medical Science, Gifu University Graduate School of Medicine, Gifu, Japan; [3]Department of Food Science, Kyoto Women's University, Kyoto, Japan and [4]Division of Gene Therapy and Regenerative Medicine, Cognitive and Molecular Research Institute of Brain Diseases, Kurume University, Kurume, Japan

Insulin-like growth factor (IGF), hepatocyte growth factor (HGF), and heparin-binding epidermal growth factor-like growth factor (HB-EGF) are cardiogenic and cardiohypertrophic growth factors. Although the therapeutic effects of IGF and HGF have been well demonstrated in injured hearts, it is uncertain whether natural upregulation of HB-EGF after myocardial infarction (MI) plays a beneficial or pathological role in the process of remodeling. To answer this question, we conducted adenoviral HB-EGF gene transduction in *in vitro* and *in vivo* injured heart models, allowing us to highlight and explore the HB-EGF-induced phenotypes. Overexpressed HB-EGF had no cytoprotective or additive death-inducible effect on Fas-induced apoptosis or oxidative stress injury in primary cultured mouse cardiomyocytes, although it significantly induced hypertrophy of cardiomyocytes and proliferation of cardiac fibroblasts. Locally overexpressed HB-EGF in the MI border area in rabbit hearts did not improve cardiac function or exhibit an angiogenic effect, and instead exacerbated remodeling at the subacute and chronic stages post-MI. Namely, it elevated the levels of apoptosis, fibrosis, and the accumulation of myofibroblasts and macrophages in the MI area, in addition to inducing left ventricular hypertrophy. Thus, upregulated HB-EGF plays a pathophysiological role in injured hearts in contrast to the therapeutic roles of IGF and HGF. These results imply that regulation of HB-EGF may be a therapeutic target for treating cardiac hypertrophy and fibrosis.
Laboratory Investigation (2005) 0, 000–000. doi:10.1038/labinvest.3700282

Keywords: apoptosis; gene transfer; growth factor; myocardial infarction; remodeling

Heparin-binding epidermal growth factor-like growth factor (HB-EGF), a member of the EGF-family of growth factors, is synthesized as a type I transmembrane protein (proHB-EGF).[1] Membrane-bound proHB-EGF is cleaved at its juxtamembrane domain by a specific metalloproteinase, resulting in shedding of soluble HB-EGF.[2] Whereas soluble HB-EGF is a potent mitogen for a number of cell types, including vascular smooth muscle cells, fibroblasts,

keratinocytes, and hepatocytes,[3–5] the activity of proHB-EGF may be mitogenic or growth inhibitory depending on cell type.[6]

HB-EGF has been implicated in a number of physiological and pathological processes. HB-EGF may play a role in the development of atherosclerosis resulting from smooth muscle cell hyperplasia,[4,7,8] pulmonary hypertension, and oncogenic transformation.[9,10] In contrast, HB-EGF is therapeutic for the skin,[11,12] kidney,[13,14] liver, and small intestine.[3,5,15,16] HB-EGF is markedly upregulated during the acute phase of injury and plays an essential role in epithelial cell repair, proliferation and regeneration in these organs.[5,11,13,15,17] Further direct evidence of therapeutic benefit was provided by studies of administration of recombinant HB-EGF

2

in animal ischemic disease models.16 Thus, HB-EGF plays a number of physiological roles, and its effects are diverse and even opposing in nature depending on the tissues examined.

It has been observed that HB-EGF-null mice develop severe heart failure associated with dilated ventricular chambers, diminished cardiac function, and grossly enlarged cardiac valves,[18,19] indicating that HB-EGF is an essential cardiogenic factor. HB-EGF is found in the adult heart under normal physiological conditions,[20] and the HB-EGF and/or EGF receptor (EGFR) families are further upregulated under pathological conditions such as cardiac hypertrophy[21] or myocardial infarction (MI).[22,23] Together with the recent finding that shedding of proHB-EGF results in cardiac hypertrophy,[24] it has recently been suggested that HB–EGF-induced cardiomyocyte hypertrophy plays a central role in hypertensive heart disease.[24,25] However, several previous studies demonstrated that overexpression of hepatocyte growth factor (HGF) and insulin-like growth factor (IGF), which are also cardiogenic growth factors, significantly induced cardiac hypertrophy but had potent therapeutic rather than pathologic effects in injured hearts, including those damaged by MI.[26–29] This led us to question whether HB-EGF might also possess therapeutic activity in the injured heart. Intriguingly, were HB-EGF to prove pathogenic, it could be the result of a secondary biological effect of this molecule separate from its promotion of hypertrophy. Thus, we endeavored to settle the questions raised by these conflicting reports in the most direct way possible, through targeted overexpression of HB-EGF in heart lesions.

One obvious approach by which to overexpress a target gene and explore the resulting effects would be to use transgenic mouse (TgM) technology, currently one of the most powerful approaches to elucidate directly the physiological and pathological roles of a gene of interest. In the present study, we opted instead to use an adenoviral gene transduction strategy, which allowed us to answer the same biological question while at the same time enabling a first assessment of the use of HB-EGF in gene therapy. Additionally, the use of an adenoviral vector allowed for greater spatial and temporal control of HB-EGF expression compared with the TgM approach, as persistent overexpression of the transgene (from the embryonic stage and before the onset of a disorder) may have produced data artefacts. Previous studies demonstrated that the expression of HB-EGF and EGFR family mRNAs was significantly increased around MI lesions.[22,23] In this context, adenoviral HB-EGF gene transduction around the MI area following onset of MI may serve to highlight the effect of HB-EGF on both cardiomyocytes and noncardiomyocytes following MI, offering a means to elucidate the role of this intriguing molecule in the development of heart disease.

Materials and methods

Recombinant Adenoviral Vectors

Replication-defective recombinant adenoviral vectors (Ads), Ad.HB-EGF and Ad.LacZ, which express HB-EGF or LacZ gene under the transcriptional control of a Rous sarcoma virus long-terminal repeat, were constructed as described previously.[27,30,31] All Ads were amplified in 293 cells, purified twice on CsCl gradients, and desalted.[27,30,31]

Injury Models in Primary Cultured Cardiomyocytes and Cardiac Fibroblasts

Cardiomyocytes and cardiac fibroblasts were isolated from 1-day-old neonatal Balb/c mice as previously reported.[32] The cardiomyoctes were incubated in Dulbecco's modified Eagle's medium (D-MEM, Sigma Chemical Co., St Louis, MO, USA) containing 5% fetal bovine serum (Sigma Chemical Co.) at 37°C for 24 h, and subsequently infected with Ads at various multiplicities of infection (MOI), followed by incubation in serum-free D-MEM for 48 h. In injury models of apoptosis and oxidative stress, cells were incubated with either $1 \mu g/ml$ agonistic anti-Fas antibody[33] (Jo2, Beckton-Dickinson Biosciences, San Jose, CA, USA) with $0.05 \mu g/ml$ actinomycin D (Sigma Chemical Co.) for 24 h, or with $100 \mu M$ H_2O_2 (Wako Pure Chemical Industry, Osaka, Japan) for 1 h as previously described.[34,35] Cell viability was determined by WST-8 assay (Dojindo, Kumamoro, Japan) in accordance with the manufacturer's protocol 24 h after the induction of cell death.

For proliferation assays, cardiac fibroblasts were incubated in D-MEM supplemented with 5% fetal bovine serum, and were used following three or four passages. The purity of these cultures was >95% cardiac fibroblasts as confirmed by vimentin-positive, desmin-negative and α-smooth muscle actin-negative stainings as previously described.[36] WST-8 assay was performed at 24, 48 and 72 h after infection with Ads or addition of recombinant human HB-EGF (R&D Systems Inc., Minneapolis, MN, USA).

Immunocytochemistry and Analysis of Primary Cultured Cardiomyocytes

At 24 h following adenoviral infection at MOI 30, primary cultured cardiomyocytes were fixed in 4% paraformaldehyde, permeabilized with 0.05% Triton-X and stained with primary goat anti-human HB-EGF antibody (R&D Systems Inc.), secondary donkey anti-goat IgG Alexa 488 antibody (Molecular Probes, Inc., Eugene, OR, USA), rhodamine phalloidin (Molecular Probes, Inc.) and Hoechst 33342 (Molecular Probes, Inc.). Digital images captured using a laser-confocal microscope system (LSM510, Carl Zeiss, Oberkochen, Germany) were employed

for morphometric and quantitative analyses using Adobe Photoshop 7.0 software (Adobe Systems Inc., San Jose, CA, USA).

Animal Studies

Male Japanese white rabbits weighing 2–2.5 kg underwent a 30-minute occlusion of the left coronary artery, followed by reperfusion, in order to generate MI as previously described.[37] Ad.HB-EGF or control Ad.LacZ (1 × 10^{11} viral particles) (each group, $n = 16$) was directly injected into the border area between the risk and the intact areas at the time of reperfusion. Echocardiograms were recorded just before and 2 or 4 weeks after generation of MI. The rabbits were killed either 2 or 4 weeks later (each, $n = 8$) and the hearts were collected, weighed, and then processed to obtain histological sections. In the sham control group ($n = 4$), the chests of the rabbits were opened and closed under anesthesia without occlusion of the coronary artery or adenoviral injection, and echocardiograms and histological analyses were performed 2 or 4 weeks later. All animal studies were performed in accordance with the guidelines of the National Institute of Health as dictated by the Animal Care Facility at the Gifu University School of Medicine.

Adenoviral Gene Transduction Efficiencies and X-Gal Staining

The efficiency of in vitro and in vivo adenoviral gene transduction was analyzed by Ad.LacZ infection and X-gal staining, as previously described.[27,30,31]

Pathological Examination in Animal Experiments

The estimation of the risk and MI areas has been described previously.[37] Briefly, the coronary branch in the excised heart was reoccluded and 4% Evans blue dye (Sigma Chemical Co.) was injected via the aorta to determine the risk area. The LV was sectioned into seven slices parallel to the atrioventricular ring. Each slice was incubated in 1% solution of triphenyl tetrazolium chloride (TTC) to visualize the infarct area.

For histological analysis, the heart was fixed in 10% formalin and embedded in paraffin, and 4-μm sections were stained with hematoxylin and eosin (H–E) or Masson's trichrome for regular or fibrotic estimation, respectively. The sizes of individual cardiomyocytes were measured using the LUZEX F system (Nireco, Kyoto, Japan). Apoptotic cells were detected under light microscopy by terminal deoxynucleotidyl transferase-mediated deoxyuridine triphosphate biotin nick end labeling (TUNEL) assay (ApopTag kit, Intergen Co., Purchase, NY, USA) in accordance with the manufacturer's protocol. The immunohistochemical staining for proliferating

cells, α-smooth muscle actin (SMA), rabbit macrophages and vascular endothelial cells were carried out with anti-Ki-67 (MIB-1, Dako), anti-SMA (1A4, Dako), anti-RAM11 (Dako) and anti-CD31 (JC/70A, Dako) antibody, respectively, as described previously.[37] For fluorescent immunohistochemistry and TUNEL assay, 6-μm frozen sections were fixed in 4% paraformaldehyde and stained using a fluorescein-FragEL DNA fragmentation detection kit (Oncogene Research Products, San Diego, CA, USA) together with individual antibodies, according to the manufacturer's instructions.

Statistical Analysis

Data are represented as means ± standard error of the mean. Statistical significance was determined using Student's t-test. One-way ANOVA was used in multiple comparisons. $P < 0.05$ was considered to be statistically significant. All statistical analysis was performed with StatView software (SAS Institute Inc., Cary, NC, USA).

Results

Adenoviral Gene Transduction Efficiency In Vitro

The adenoviral constructs demonstrated high infectivity in primary cultured mouse cardiomyocytes; infection of cardiomyocytes with Ad.LacZ at MOIs of 10 and 30 resulted in approximately 80% and over 90% successful gene transduction, respectively, without morphological changes, cell damage or death (Figure 1). Cardiac fibroblasts also demonstrated high infectivity, although the accurate quantification was difficult.

Effects of Adenoviral HB-EGF Gene Transduction on Cardiomyocytes and Cardiac Fibroblasts In Vitro

To explore the direct effects of HB-EGF on cardiomyocytes, we examined cell viability following Ad.HB-EGF infection in two representative injury models of primary cultured cardiomyocytes, Fas-induced apoptosis[34,35] and H_2O_2 oxidative stress injury[34,35] (Figure 2a and b). Both types of stimulus at the predetermined doses efficiently induced cell death in approximately 80% of the cultured cells, and adenoviral HB-EGF gene transduction did not result in significant changes in viability in either of these models at any MOI (Figure 2a and b). However, cardiomyocytes became significantly enlarged, and their F-actin-containing myofibrils were drastically condensed, enlarged and increased in number following adenoviral HB-EGF gene transduction (Figures 3 and 4).

Next, we explored whether HB-EGF exhibited an inhibitory or stimulatory effect on the growth of cardiac fibroblasts. Both the addition of recombinant HB-EGF and adenoviral HB-EGF gene transduction
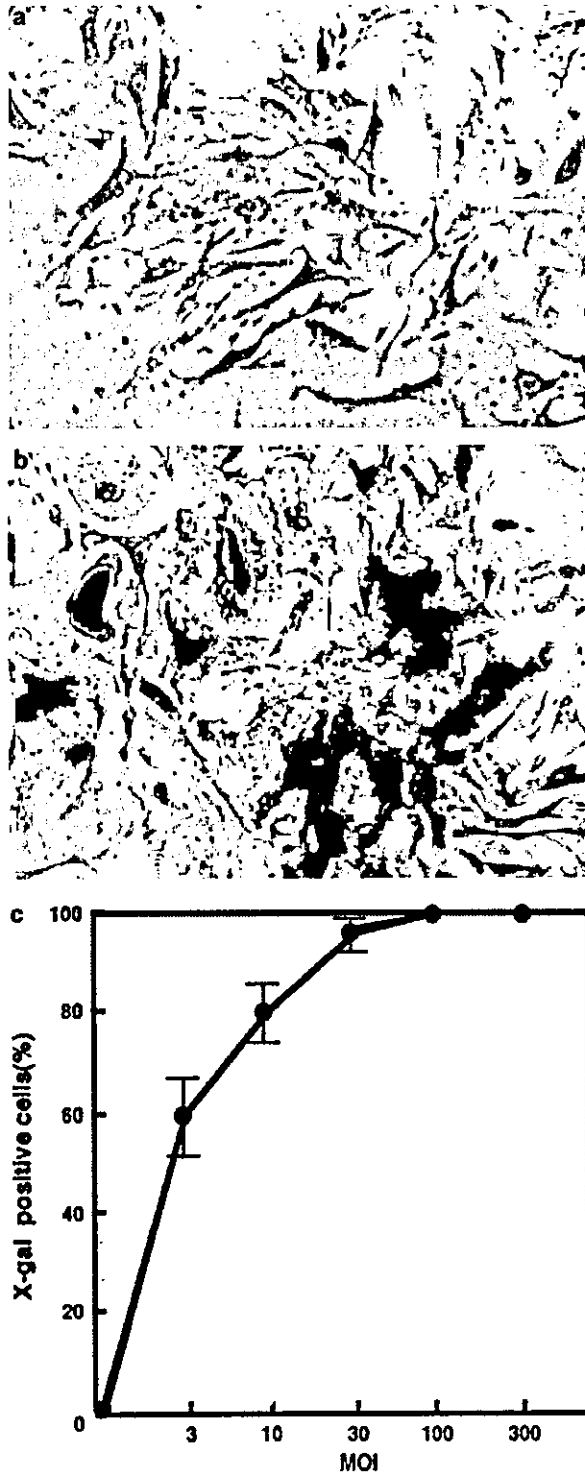
Figure 1 Efficiency of adenoviral gene transduction in primary cultured mouse cardiomyocytes. X-gal staining after Ad.LacZ infection at (a) MOI 0 (ie, no infection as a negative control) and (b) MOI 10. (c) Graph showing adenoviral gene transduction efficiency at various MOIs.
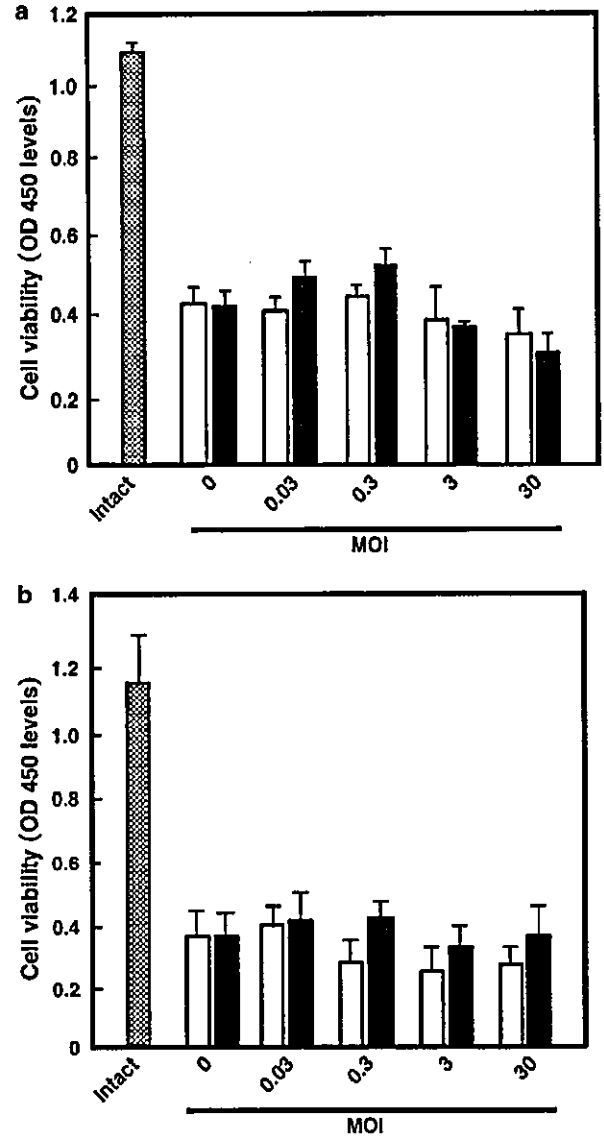

Figure 2 Cell viability after adenoviral HB-EGF gene transduction in two injury models of primary cultured cardiomyocytes. Primary cultured cardiomyocytes were infected with Ad.LacZ (white bar) or Ad.HB-EGF (black bar), and were then exposed to 1 μg/ml anti-Fas antibody and 0.05 μg/ml actinomycin D for 24 h (a) or 100 μM H_2O_2 for 1 h (b); cell viability was evaluated by WST-8 assay. 'Intact' indicates the control (untreated cells).

significantly accelerated the growth of cardiac fibroblasts. (Figure 5). Thus, HB-EGF gene transduction and overexpression conferred a direct hypertrophic effect on cardiomyocytes and a growth-stimulating effect on cardiac fibroblasts, but did not have additive death-inducible or cytoprotective effects on cardiomyocytes.
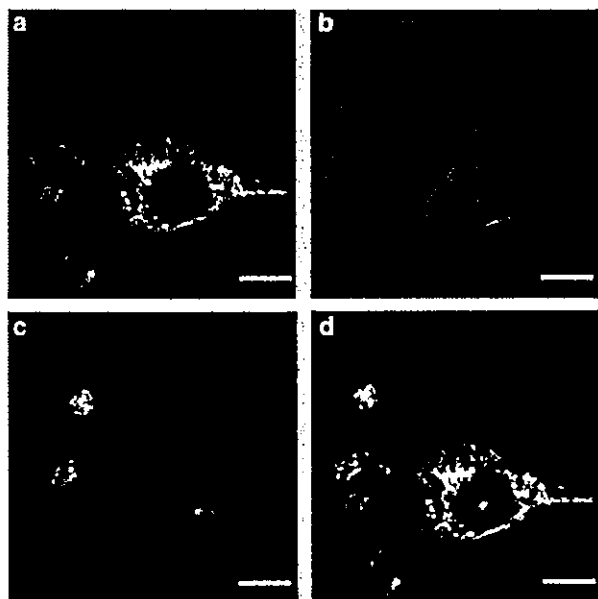
Figure 3 Microscopic images of HB-EGF gene-transduced cardiomyocytes. Confocal microscopic analysis demonstrated apparent hypertrophic changes in individual cardiomyocytes overexpressing HB-EGF after Ad.HB-EGF infection at MOI 30. (a) Staining with goat anti-human HB-EGF antibody and Alexa 488-labeled donkey anti-goat secondary antibody, (b) staining using rhodamine phalloidin-labeled F-actin, (c) staining using Hoechst 33342 (nuclei), and (d) merged image. Scale bar = 20 μm.
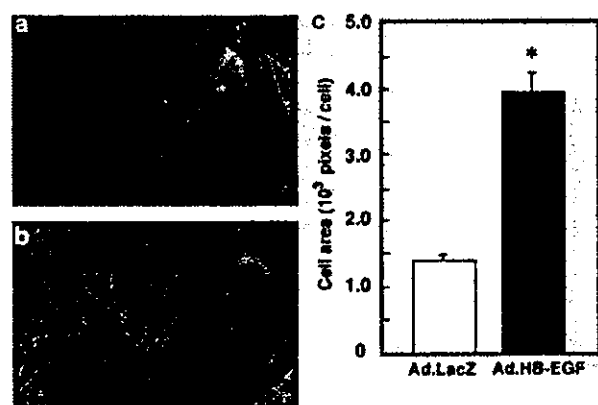

Figure 5 Proliferation of cardiac fibroblasts overexpressing HB-EGF. Cardiac fibroblasts (cell density; 1 x 10⁵/ml) were infected with Ad.LacZ at MOI 30 (shaded bar) or Ad.HB-EGF at MOI 30 (black bar), or were exposed to 10 or 20 ng/ml rHB-EGF for 24, 48, and 72 h; cell proliferation was evaluated by WST-8 assay at OD 450 nm. *P<0.05.

Figure 4 Morphometric and quantitative analysis of HB-EGF gene-transduced cardiomyocytes. (a) Hypertrophy of cardiomyocytes after Ad.HB-EGF infection at MOI 30. (b) Hypertrophy as shown by condensation of rhodamine phalloidin-labeled F-actin and enlargement of cell area. Original magnification, x 100. (c) Graphic depiction of cell area determined for 500 cardiomyocytes infected with Ad.HB-EGF or Ad.LacZ. *P<0.001.

Macroscopic Findings after Adenoviral HB-EGF Gene Transduction in the Rabbit MI Model

Recent studies have demonstrated that HB-EGF and EGFR family mRNAs were significantly upregulated around MI lesions,[22,23] and it is for this reason that
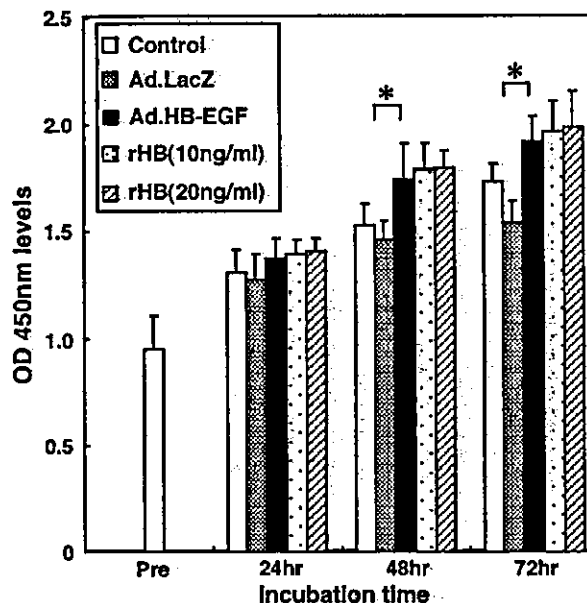
we injected our adenovirus constructs specifically into this region. X-gal staining after Ad.LacZ injection into this area showed that we were able to drive gene transduction predominantly around the MI (Figure 6a). A number of previous studies have demonstrated retention of transgene expression for at least 3 weeks following in vivo adenoviral gene transduction into the heart.[38–40] We have previously described the pathological process in the rabbit MI model in detail, including granulation consisting of myofibroblasts, macrophages and neovasculation at 2 weeks (the subacute stage) and scar formation at 4 weeks (the chronic stage).[37] Together, these results suggested that the period of transgene expression resulting from adenoviral gene transduction would be sufficient for the purposes of this study. In this context, we injected Ad.HB-EGF into the MI injury border area, estimated the risk area and the MI area by TTC and Evans blue dye after 2 weeks (as shown in Figure 6b) and ultraechographically analyzed cardiac function 2 and 4 weeks later. There was no difference in risk area between the two groups (Figure 6c). On the other hand, the ratio of MI area to risk area was seemingly reduced to a small degree by Ad.HB-EGF at 2 weeks post-injection due to hypertrophic changes; however, this reduction was not statistically significant (HB-EGF; 19.6±3.5% vs LacZ; 24.6±2.9%, P=0.277) (Figure 6d).
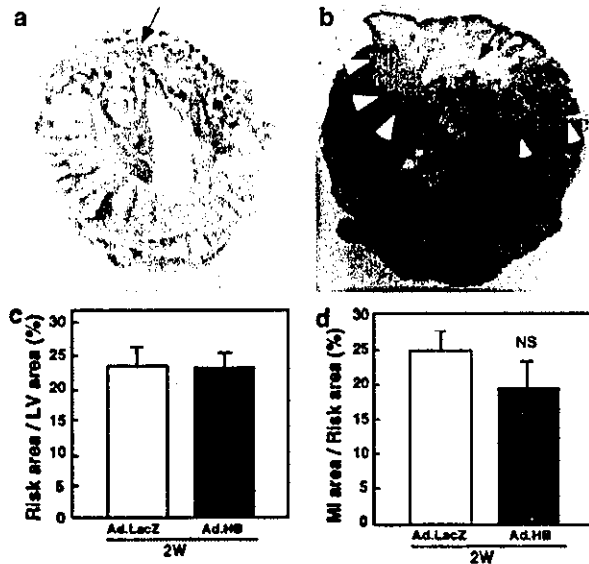
6

Figure 6 Macroscopic findings after adenoviral HB-EGF gene transduction in a rabbit MI model. (a) X-gal staining after Ad.LacZ injection into the border area. The arrow indicates the infarcted area. (b) Triphenyl tetrazolium chloride (TTC) and Evans blue staining define the risk areas (arrowheads), MI areas (arrow), and the intact (blue) areas. Graphs showing the risk area (c) and the MI area (d). Morphometric analysis of TTC/Evans blue-stained macroscopic slides 2 weeks after MI. NS: no significant difference.

Cardiac Function and Histological Changes Following Adenoviral HB-EGF Gene Transduction in the Rabbit MI Model

Rabbits that received a control Ad.LacZ injection following MI clearly demonstrated a worsening of cardiac parameters such as left ventricular ejection fraction (LVEF) and left ventricular dimension at end-diastole (LVDd), as assessed by ultraechocardiography (UCG) at 2 and 4 weeks post-MI, compared with sham-operated rabbits that underwent neither adenoviral gene transduction nor MI (Figure 7a and b). Ad.HB-EGF injection after MI neither improved nor further worsened cardiac function, as assessed by LVEF or LVDd at 2 or 4 weeks compared with the Ad.LacZ-treated rabbits. On the other hand, anterior wall thickness (AWt) at 2 weeks (HB-EGF, 2.7±0.3 mm vs LacZ, 1.9±0.1 mm, $P<0.05$, Figure 7c) and the ratio of LV weight to body weight at 2 and 4 weeks were significantly increased by Ad.HB-EGF injection (2 weeks: HB-EGF, 1.59±0.06 vs LacZ, 1.44±0.03, $P<0.05$; 4 weeks: HB-EGF, 1.67±0.09 vs LacZ, 1.40±0.05, $P<0.05$) (Figure 7d); these findings were consistent with macroscopically observed hypertrophic changes (Figure 8). In addition, fibrosis in and around the MI area, which was induced by the MI itself, was increased by injection with Ad.HB-EGF at 2 and 4 weeks post-MI (2 weeks: HB-EGF,

7149±675 pixels vs LacZ, 4230±331 pixels, $P<0.001$; 4 weeks: HB-EGF, 6575±534 pixels vs LacZ, 4414±494 pixels, $P<0.05$) (Figure 8f).

Accordingly, histological examination revealed that individual cardiomyocytes at the border area were remarkably hypertrophic 2 and 4 weeks after Ad.HB-EGF injections (2 weeks: HB-EGF, 18.76±0.29 μm vs LacZ, 16.53±0.34 μm; $P<0.05$; 4 weeks: HB-EGF, 20.49±0.28 μm vs LacZ, 18.23±0.40 μm, $P<0.05$) (Figures 9 and 10). Thus, overexpression of HB-EGF markedly induces cardiomyocyte hypertrophy and fibrosis without affecting cardiac function, suggesting that this molecule plays an important role in accelerating the remodeling process after MI.

Characteristic Histological Findings in the MI Area

To clarify the mechanisms responsible for the enhancement of post-MI remodeling in the hearts treated with the HB-EGF gene during the subacute and chronic stages of MI, we performed histological examinations of rabbit hearts at 2 and 4 weeks post-MI. Increases in the number of cells in the MI area 2 and 4 weeks after MI were more prominent in rabbits receiving Ad.HB-EGF than in those receiving control Ad.LacZ (2 weeks: HB-EGF, 235±4 cells/field vs LacZ, 145±4 cells/field, $P<0.001$; 4 weeks: HB-EGF, 180±6 cells/field vs LacZ, 97±3 cells/field, $P<0.001$) (Figure 11a–c). Likewise, the number of proliferating (Ki-67 positive) cells increased more in the Ad.HB-EGF-treated rabbits than in those treated with Ad.LacZ (2 weeks: HB-EGF, 27.6±1.0 cells/field vs LacZ, 7.6±0.3 cells/field, $P<0.001$; 4 weeks: HB-EGF, 25.3±1.4 cells/field vs LacZ, 15.8±1.3 cells/field, $P<0.001$) (Figure 11d–f). Immunohistochemical studies demonstrated that these accumulated cells were primarily SMA-positive spindle myofibroblasts at both 2 and 4 weeks (2 weeks: HB-EGF, 62.7±0.8 cells/field vs LacZ, 38.0±0.9 cells/field, $P<0.001$; 4 weeks: HB-EGF, 48.6±1.7 cells/field vs LacZ, 22.7±1.1 cells/field, $P<0.001$) (Figure 11g–i), and RAM 11-positive macrophages at 2 weeks only (HB-EGF, 18.4±1.0 cells/field vs LacZ, 4.2±0.3 cells/field, $P<0.001$) (Figure 11j–l). On the other hand, the finding that more CD31-positive vascular endothelial cells were observed in the border area than in the remote area in both groups suggests an angiogenic effect induced by certain endogenous factors following MI (Figure 11m–o).

Interestingly, these vascular endothelial cells were not further increased by Ad.HB-EGF injections, in contrast to the significant increases observed in total cells, proliferating cells, myofibroblasts and macrophages, suggesting that HB-EGF most likely lacks angiogenic potential.
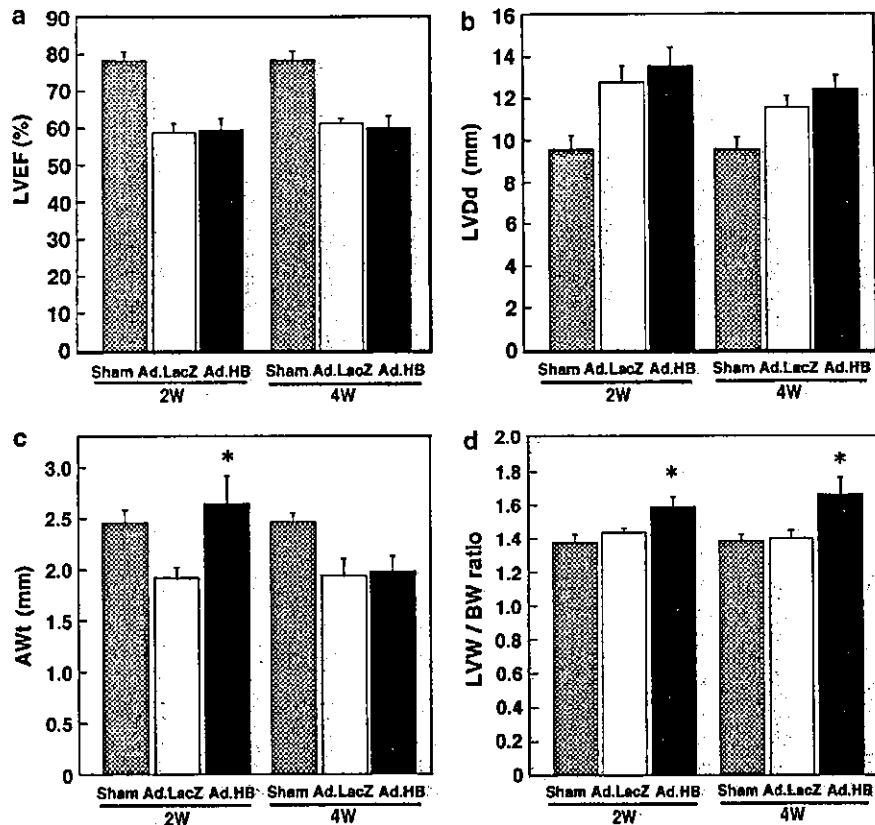
Figure 7 Echocardiographic measurements and left ventricular (LV) weight after adenoviral HB-EGF gene transduction in the postinfarct rabbit heart. Graphs showing the (a) LVEF, (b) LV size, (c) wall thickness, and (d) LV weight to body weight at 2 and 4 weeks after Ad.HB-EGF gene transduction in MI rabbits. Cardiac function parameters were assessed by echocardiographic examination. LVEF: left ventricular ejection fraction; LVDd: left ventricular dimension at end-diastole; AWt: anterior wall thickness; LVW: LV weight; BW: indicated body weight. 'Sham' indicates sham-operated rabbits without MI or adenoviral transduction. *$P<0.05$.

Apoptosis in the MI Area after Adenoviral HB-EGF Gene Transduction

To estimate apoptosis in the MI area, TUNEL staining was performed. Unexpectedly, the number of TUNEL-positive cells was increased by Ad.HB-EGF injection at 2 weeks after MI (HB-EGF, $1.95 \pm 0.10\%$ vs LacZ, $1.04 \pm 0.09\%$, $P<0.001$) (Figure 12). Notably, most of the TUNEL-positive cells were costained with the anti-RAM11 antibody (Figure 13a and b), but not with anti-SMA antibody (Figure 13c), nor by markers for cardiomyocytes such as troponin I (Figure 13d). Moreover, TUNEL-positive signals were detected in the cytoplasm of some macrophages with intact nuclei. Thus, the TUNEL-positive cells may be not only apoptotic macrophages, but also viable macrophages that had phagocytosed other apoptotic cells (Figure 13b). Thus, in vivo HB-EGF gene transduction stimulated the activation of noncardiomyocytes, including macrophages, fibroblasts and myofibroblasts, but not endothelial cells, in and around the MI area,

while at the same time inducing cardiac hypertrophy.

Discussion

This is the first study to explore directly the in vivo effects of overexpressed HB-EGF on heart remodeling after reperfused MI. In addition, our unique adenoviral gene transduction and overexpression approach allowed a preliminary assessment of the potential utility of HB-EGF in gene therapy. Overexpressed HB-EGF in the MI lesion did not result in a beneficial or therapeutic outcome, in contrast to results observed with HGF or IGF in rodent MI models, but rather exacerbated the remodeling process through the activation of specific types of noncardiomyocytes.

To identify the HB-EGF-related biological mechanism underlying heart failure, distinguishing the various phenotypic effects of HB-EGF from those of HGF and IGF may prove useful, because despite their differences all of these factors are essential
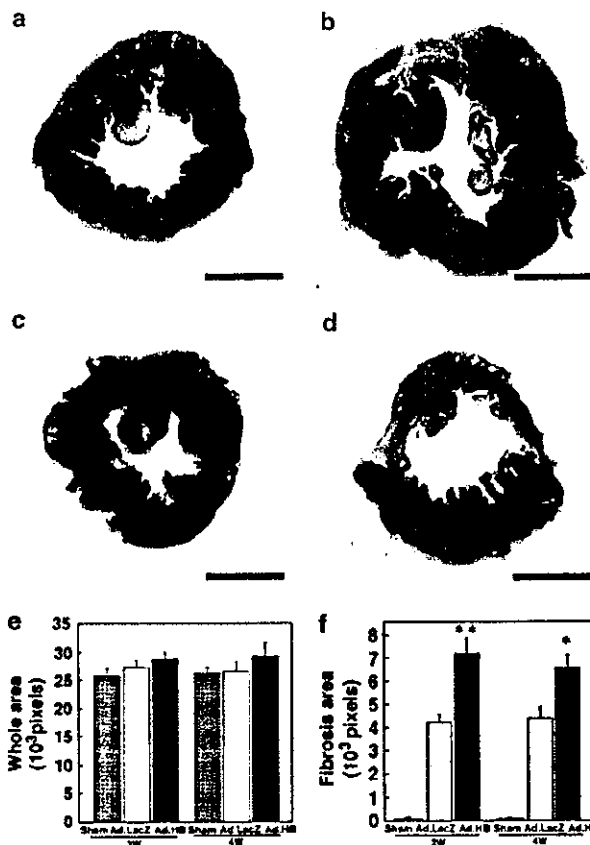
Figure 9 Histological findings at the MI border area after treatment. H–E-stained slides of LV 2 weeks post-MI. (a), (c) Ad.LacZ-treated mice and (b), (d) Ad.HB-EGF-treated mice. Squared-in areas in (a) and (b) (original magnification × 100) were magnified in (c) and (d) (original magnification × 400), respectively.

Figure 8 Macroscopic findings and histological analyses of transverse sections of hearts after adenoviral HB-EGF gene transduction. Fibrosis areas were stained blue with Masson's trichrome. (a) Ad.LacZ group (control) at 2 weeks after MI, (b) Ad.HB-EGF group at 2 weeks after MI, (c) Ad.LacZ group at 4 weeks after MI, (d) Ad.HB-EGF group at 4 weeks after MI. Graphs showing the whole areas (e) and fibrosis areas (f). The stained areas were morphometrically analyzed by counting pixels. Scale bar = 5 mm, *P < 0.05, **P < 0.001.

Figure 10 Size of cardiomyocytes at the remote and border areas of MI after treatment. The size of individual cardiomyocytes at the remote and border areas was morphometrically analyzed. *P < 0.001.

cardiogenic growth factors as well as potent inducers of cardiac hypertrophy.[27,29,41] The most important difference between HB-EGF and HGF/IGF, which accounts for the observed discrepancy, is the lack of a direct cytoprotective effect of HB-EGF on cardiomyocytes, in contrast to the potent cytoprotective effect observed for HGF and IGF in injured hearts.[27,29,41] This is a unique feature of HB-EGF, because most organogenic and/or organotrophic growth factors exert direct antiapoptotic effects, for example, HGF or IGF in mouse or rat cardiomyocytes[26–29] and HB-EGF in the small intestine,[42] In this regard, future studies to explore the differences among the molecules and signal transduction pathways involved in the activity of each growth factor would be biologically important.

Another important feature that differentiated HB-EGF from HGF and IGF was its observed lack of angiogenic activity. It should be noted that improve-
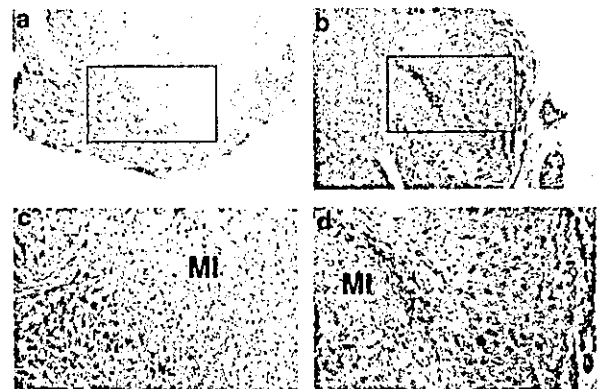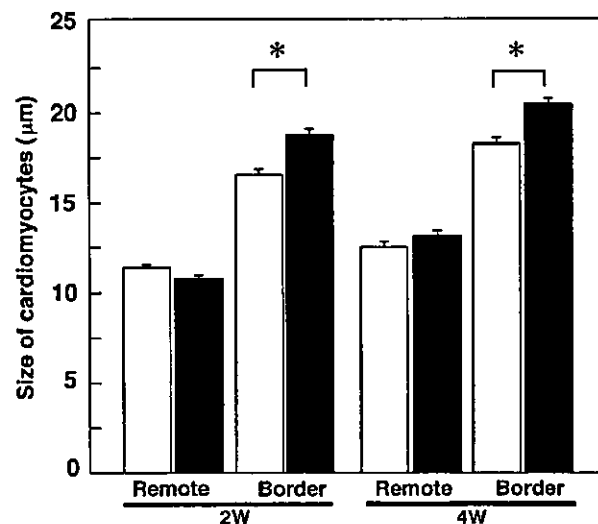
ment of cardiac dysfunction after MI has been successfully achieved by gene therapy using angiogenic factors that do not directly act on cardiomyocytes.[29,43] This fact suggests that angiogenesis plays a crucial role in postinfarction remodeling, and that the absence of an angiogenic effect of overexpressed HB-EGF may be largely responsible for its lack of therapeutic action.

In addition, HB-EGF was revealed to have a mitogenic effect on fibroblasts, in contrast to the potent antifibrotic effect of HGF following MI.[27] Moreover, the characteristic finding after HB-EGF
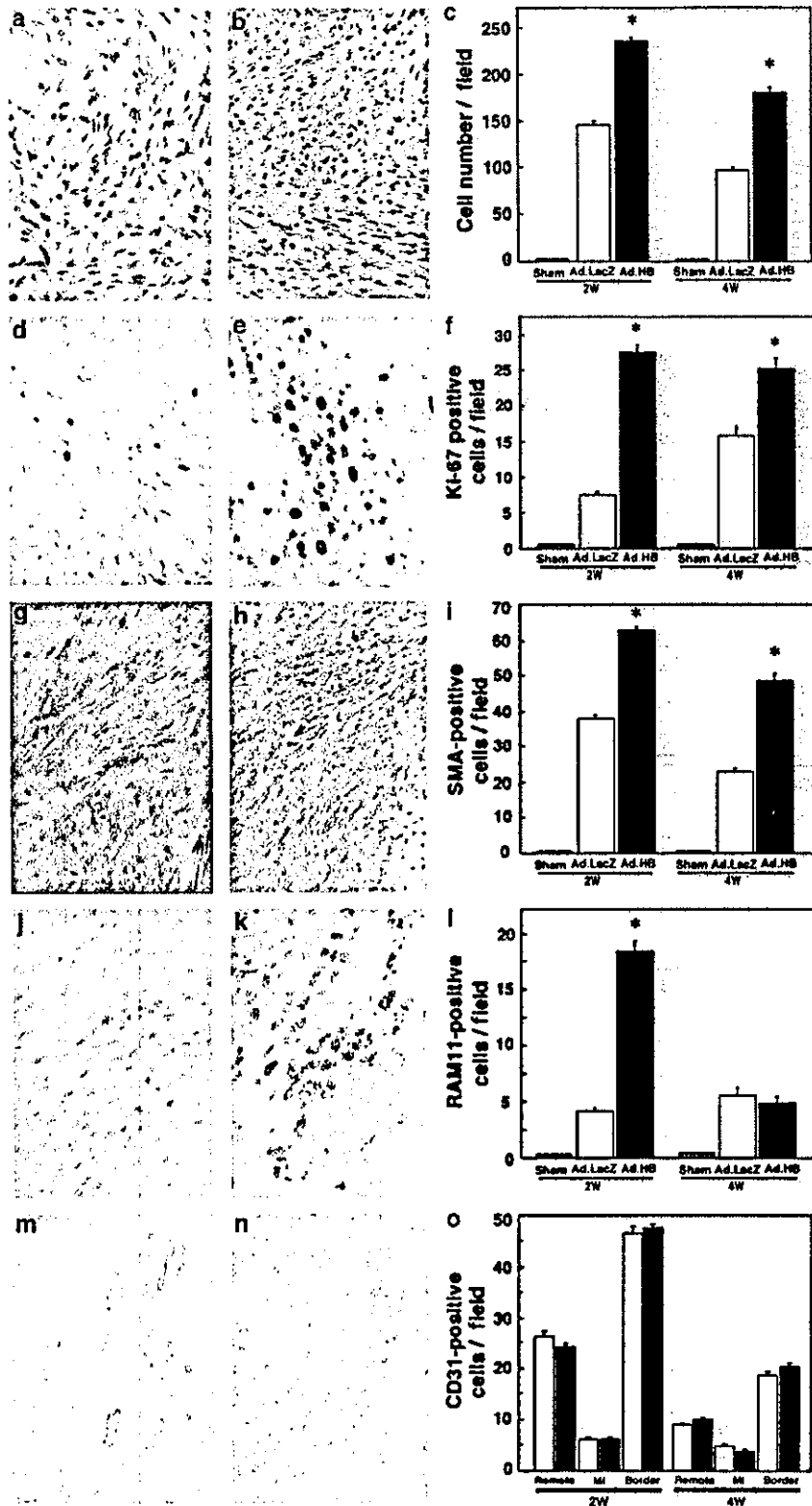
Figure 11 Histological and immunohistochemical findings in the MI area post-treatment. (a, b) H–E-stained-tissues, and immunohistochemically stained-tissues using (d, e) anti-Ki-67, (g, h) anti-SMA, (j, k) anti-RAM11, or (m, n) anti-CD31 antibodies 2 weeks after MI are shown (original magnification, × 400 for a, b, d, e, g, h, j and k, and × 100 for m and n). The number of positive cells in the field 2 and 4 weeks after MI were calculated and shown in the graphs (c, f, i, l, and o). *$P < 0.001$.
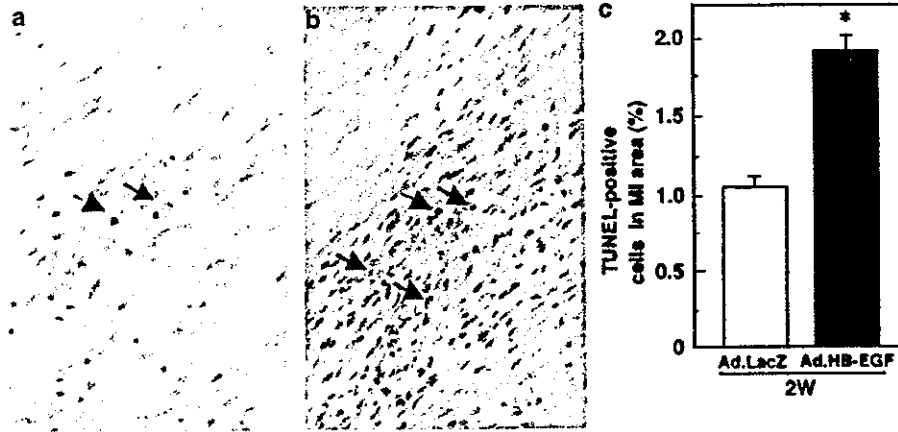
Figure 12 TUNEL staining in the MI area. TUNEL-positive cells (arrows) in the MI area 2 weeks after each treatment are shown. (a) and (b) indicate Ad.LacZ- and Ad.HB-EGF-treated mice, respectively. (c) The percentage of TUNEL-positive cells in the MI area was calculated by morphometric and quantitative analyses . $*P < 0.001$.
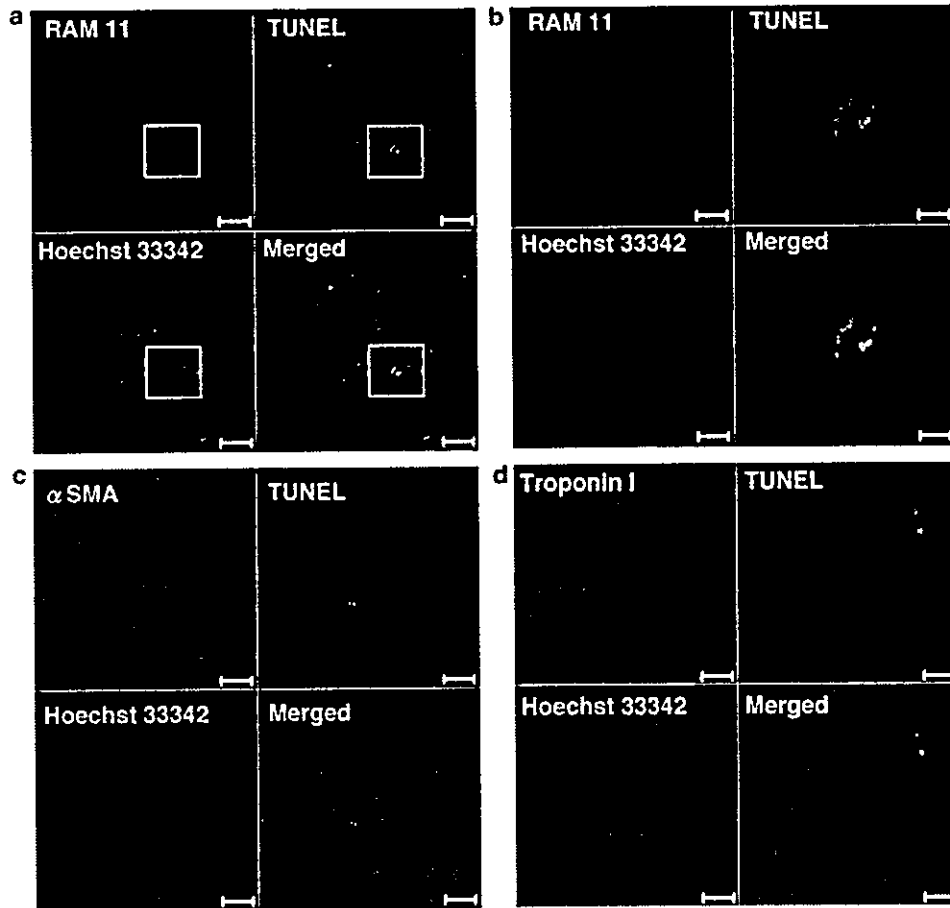

Figure 13 Immunofluorescent-TUNEL staining in the MI area. Laser confocal-microscopic analysis of slides that were triple-stained with TUNEL and (a, b) anti-RAM11, (c) anti-SMA and (d) anti-troponin I antibodies, and Hoechst 33342. Squared areas within (a) were magnified and shown in (b). Scale bars, 20 μm (a, c, d) and 5 μm (b).

gene transduction was prominent accumulation of SMA-positive myofibroblasts and macrophages in the MI-affected areas. We previously reported that the infiltrating cells at the subacute stage post-MI were primarily macrophages, endothelial cells, and myofibroblasts, and that all of these cell types were

entering apoptosis at an elevated rate.[37] Thus, the previously unknown factor that activates fibroblasts, myofibroblasts, and macrophages during post-infarction remodeling is now strongly suggested to be HB-EGF. Taken together with the lack of an agonistic death-inducible effect of HB-EGF directly on cardiomyocytes, pathologically upregulated HB-EGF may be responsible for activating these specific types of noncardiomyocytes, thus exacerbating post-MI remodeling.

The detailed molecular mechanisms by which HB-EGF activates these specific types of noncardiomyocytes remain to be elucidated. It was previously reported that HB-EGF stimulated the mitogenic and motogenic activities of smooth muscle cells,[4,7] and also that it reduced the expression of SMA in fibroblasts.[17] HB-EGF may play a regulatory role in the growth of fibroblasts and their transformation to myofibroblasts in the heart, as was suggested for the postinfarct kidney.[17] However, the biological relationship between HB-EGF and macrophages has yet to be studied, so future work to explore these molecular mechanisms would be interesting and fruitful. In this study, the overexpressed HB-EGF may consist not only of soluble HB-EGF, a potent mitogen for diverse cell types, but also membrane-bound proHB-EGF, whose functions may be diverse depending on cell types. In this context, future biological studies comparing the physiological and pathological effects of proHB-EGF on the heart with those of soluble HB-EGF may be of interest, although a suitable experimental system should be carefully established.

Finally, the recent finding that shedding of proHB-EGF resulted in cardiac hypertrophy suggests that upregulated HB-EGF might play a central role in hypertensive heart diseases.[24,25] However, overexpression of HGF and IGF induced cardiac hypertrophy, but inconsistently exhibited potent therapeutic and beneficial effects on the injured heart, including that damaged by MI.[27-29] Taken together with these facts, HB-EGF-induced cardiac hypertrophy may not be a sole or direct source of pathogenesis in MI, even though cardiac hypertrophy may, in fact, be involved in specific types of heart failure. In this context, the present results importantly imply that HB-EGF-induced exacerbation of remodeling may be a novel pathological mechanism for MI.

In conclusion, upregulated HB-EGF plays a pathological role in MI by activating specific types of noncardiomyocytes, leading to exacerbation of remodeling after MI. This novel fact may be useful for developing new therapeutics as well as for elucidating the mechanism of different types of heart failure, including MI.

Acknowledgement

References

1 Higashiyama S, Abraham JA, Miller J, et al. A heparin-binding growth factor secreted by macrophage-like cells that is related to EGF. Science 1991;251:936–939.
2 Prenzel N, Zwick E, Daub H, et al. EGF receptor transactivation by G-protein-coupled receptors requires metalloproteinase cleavage of proHB-EGF. Nature 1999;402:884–888.
3 Ito N, Kawata S, Tamura S, et al. Heparin-binding EGF-like growth factor is a potent mitogen for rat hepatocytes. Biochem Biophys Res Commun 1994;198:25–31.
4 Higashiyama S, Abraham JA, Klagsbrun M. Heparin-binding EGF-like growth factor stimulation of smooth muscle cell migration: dependence on interactions with cell surface heparan sulfate. J Cell Biol 1993;122:933–940.
5 Kiso S, Kawata S, Tamura S, et al. Liver regeneration in heparin-binding EGF-like growth factor transgenic mice after partial hepatectomy. Gastroenterology 2003;124:701–707.
6 Iwamoto R, Mekada E. Heparin-binding EGF-like growth factor: a juxtacrine growth factor. Cytokine Growth Factor Rev 2000;11:335–344.
7 Miyagawa J, Higashiyama S, Kawata S, et al. Localization of heparin-binding EGF-like growth factor in the smooth muscle cells and macrophages of human atherosclerotic plaques. J Clin Invest 1995;95:404–411.
8 Kalmes A, Daum G, Clowes AW. EGFR transactivation in the regulation of SMC function. Ann NY Acad Sci 2001;947:42–54; discussion 54–45.
9 Lemjabbar H, Basbaum C. Platelet-activating factor receptor and ADAM10 mediate responses to Staphylococcus aureus in epithelial cells. Nat Med 2002;8:41–46.
10 Fu S, Bottoli I, Goller M, et al. Heparin-binding epidermal growth factor-like growth factor, a v-Jun target gene, induces oncogenic transformation. Proc Natl Acad Sci USA 1999;96:5716–5721.
11 Marikovsky M, Breuing K, Liu PY, et al. Appearance of heparin-binding EGF-like growth factor in wound fluid as a response to injury. Proc Natl Acad Sci USA 1993;90:3889–3893.
12 Tokumaru S, Higashiyama S, Endo T, et al. Ectodomain shedding of epidermal growth factor receptor ligands is required for keratinocyte migration in cutaneous wound healing. J Cell Biol 2000;151:209–220.
13 Nguyen HT, Bride SH, Badawy AB, et al. Heparin-binding EGF-like growth factor is up-regulated in the obstructed kidney in a cell- and region-specific manner and acts to inhibit apoptosis. Am J Pathol 2000;156:889–898.
14 Sakai M, Zhang M, Homma T, et al. Production of heparin binding epidermal growth factor-like growth factor in the early phase of regeneration after acute renal injury. Isolation and localization of bioactive molecules. J Clin Invest 1997;99:2128–2138.